

# Preparation and Performance Characterization of Polyimide-based Graphite Films

Kunfeng Wang<sup>1,\*</sup>

<sup>1</sup> School of Materials and Chemistry, University of Shanghai for Science and Technology, Shanghai 200093, China

\*Corresponding author: Kunfeng Wang (Email: 18322485092@163.com)

**Abstract:** With the large-scale application and high-speed operation of electronic devices, the problem of heat diffusion puts forward higher and higher requirements for effective heat dissipation materials. In this paper, chemical imidization is used to prepare polyimide (PI) films, and then carbonization and graphitization are carried out to prepare high thermal conductivity flexible graphite films. The results show that chemically imidized PI (CIPI) films have higher tensile strength, thermal stability and imidization degree than thermally imidized PI (TIPI) films. The graphite film prepared from CIPI film has a more complete crystal orientation and ordered arrangement. When the amount of chemical catalyst is 0.6%, the thermal conductivity of CIPI graphitized film is  $1597 \text{ W} \cdot \text{m}^{-1} \cdot \text{K}^{-1}$ . The high thermal conductivity is due to the large in-plane grain size and high crystal integrity. High-quality PI films can be preferentially prepared by the chemical imidization method, and then graphite films with excellent performance can be prepared.

**Keywords:** Polyimide, Chemical imidization, Carbonization, Graphitization, Thermal conductivity.

## 1. Introduction

With the development of microelectronic devices towards miniaturization and high-density integration, electronic information products tend to feature compact structures and efficient operations. Some issues emerged in this domain, such as local excessive heat generation, insufficient heat dissipation, and poor high-temperature resistance. The accumulated heat seriously affect the normal operation of electronic devices and the stability of the system<sup>[1-5]</sup>. According to the report, electronic devices require three times more heat dissipation in 5G than in 4G<sup>[6]</sup>. To address this problem, people develop thermal conductive materials mainly based on carbon-based materials that have a high heat dissipation coefficient and are lightweight. Among them, graphite films demonstrate obvious advantages in microelectronics packaging and integration due to their excellent thermal conductivity, electrical conductivity, and thinness.

There are four commonly employed methods for preparing thermally conductive graphite films: the graphene oxide (GO) reduction method (solution chemical method)<sup>[7-10]</sup>, the expanded graphite rolling method<sup>[11,12]</sup>, the vapor deposition method<sup>[13,14]</sup>, and the carbonization and graphitization of polyimide (PI) films<sup>[15,16]</sup>. K.S.etal.<sup>[10]</sup> reviewed the restoration of the graphitic structure of GO through defect repair during thermal reduction and summarized the morphology, structure, and electrical properties of GO films. They found that controlling the oxidation of graphite to synthesize GO while retaining the carbon framework is a favorable strategy, so the reduction process might not require extremely high annealing temperatures. Furthermore, it is essential to focus more on controlled oxidation without sacrificing GO production and simultaneous deoxygenation to restore the graphite structure. Y.H. Liu et al.<sup>[11]</sup> introduced  $(\text{NH}_4)_2\text{S}_2\text{O}_8$  into expanded graphite to prepare a thermally conductive film that can be bent 800 times and has a thermal conductivity of  $854 \text{ W}/(\text{m} \cdot \text{K})$ .  $(\text{NH}_4)_2\text{S}_2\text{O}_8$  was reported to act as a gas expansion and weak oxidizing agent. H.J. Park et

al.<sup>[13]</sup> investigated the structure, electrical, mechanical, and optical properties of a few layers of graphene synthesized by chemical vapor deposition on nickel-plated substrates. The PI-based graphite film obtained through carbonization-graphitization has also been extensively studied, and its thermal conductivity can currently reach  $1950 \text{ W}/(\text{m} \cdot \text{K})$ . The precursor of PI has a clear molecular structure, a high carbon yield, good thermal stability, and a wide range of sources<sup>[17,18]</sup>.

As early as in the 1990s, the carbonization-graphitization process of PI (Kapton, Uplix and Novax) with different structures has been investigated<sup>[19-21]</sup>. Many researchers have examined the effects of the monomer<sup>[22,23]</sup>, thickness<sup>[20,24]</sup>, heating rate<sup>[25]</sup>, imidization process constraints<sup>[23,26]</sup>, addition of fillers<sup>[27,28]</sup> and others on the polyimide graphite film. Although the PI-based graphite film has been studied for a considerable time, there are still numerous issues to be explored, such as: the thermal conductivity to be enhanced, the thickness range to be expanded, the catalyst to be updated, the energy consumption to be reduced, the production to be scaled up, and so forth. **Fig. 1** shows the preparation process of the graphite film.

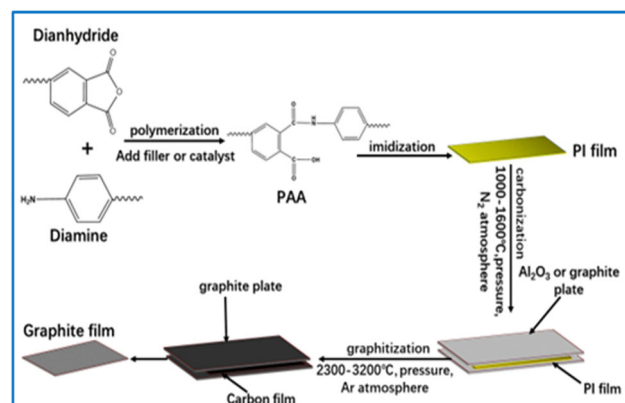


**Figure 1.** Schematic diagram of the preparation process of PI-based graphite film.

## 2. Experimental Section

### 2.1. Drugs and instruments

N, N-Dimethylacetamide (DMAc), analytical pure, from Sinopharm; 4,4'-Diaminodiphenyl ether (ODA), 99%, from Aladdin; Pyromellitic dianhydride (PMDA), 99%, from Aladdin; Phosphorus pentoxide, from Sinopharm; Isoquinoline, from Sinopharm.

Precision electronic balance XS105 Mettler Toledo; Blast drying oven XCT-1 Shanghai Suopu Instrument Co., Ltd.; Magnetic stirrer 84-1 magnetic stirrer Shanghai Meiyongpu Instrument and Meter Manufacturing Co., Ltd.;

Circulating water multi-purpose vacuum pump SHZ-DIII Shanghai Lichen Bangxi Instrument Technology Co., Ltd.; Power-increasing electric stirrer JJ-1 Changzhou Guoyu Instrument Manufacturing Co., Ltd.; Vacuum/atmosphere box furnace SX-G03133Q Tianjin Zhonghuan Electric Furnace Co., Ltd.; High-temperature graphitization furnace KGPS-100 Zhuzhou Chenxin Medium and High Frequency Equipment Co., Ltd.; Electric double-roll mill MR-100A Hefei Kejing Materials Technology Co., Ltd.; Thickness gauge Flat-head thickness gauge Shenzhen Yuanhengtong Technology Co., Ltd.; X-ray diffractometer D8 Advance Bruker; Fourier transform infrared spectrometer Spectrum 100 Perkin Elmer; Laser Raman spectrometer LabRAM HR Evolution Horiba; Thermogravimetric analyzer Pyris 1 Perkin Elmer; DSC TA Q2000 Netzsch; Laser flash instrument LFA467 Netzsch; Infrared thermal imager Compact Pro SmartSensor; 2.5KN universal material testing machine Z2.5TH Zwick/Roell; Flexing resistance tester RS-6310 Huayi Chuanghong Instrument Co., Ltd.; Four-probe tester RTS-9 4 PROBES TECH; Coating instrument Q150TES Quorum; Field emission scanning electron microscope Quanta FEG450 FEI.

### 2.2. Preparation of graphite films

Figure 2 shows the preparation process of the graphite film in this experiment. PMDA and ODA were dissolved in the DMAc solvent to prepare a PAA solution with a solid weight content of 18%. A certain content of isoquinoline was added to the PAA solution and stirred evenly at room temperature. The PAA solution was defoamed under vacuum and cast onto a glass plate to form a film, and then placed in an oven and kept at 80°C, 120°C, and 160°C for 30 minutes respectively to evaporate the solvent. After the temperature continued to rise, it was kept at 220°C, 260°C, and 300°C for 10 minutes respectively for full imidization to obtain the PI film. The PI film was placed in a nitrogen atmosphere, and the high-temperature furnace was heated from room temperature to 400°C in 30 minutes, and then heated to 480°C at a rate of 2°C/min and kept for 30 minutes. Then, it was kept warm for 60 minutes. It continued to be heated to 800°C at a rate of 1°C/min and kept for 30 minutes. Then, it was heated to 1000°C. Finally, it was cooled to 800°C at a rate of 5°C/min, and then taken out after natural cooling to obtain the PI-based carbon film. The PI-based carbon film was placed in an argon atmosphere. The high-temperature furnace was heated from room temperature to 1600°C at a rate of 10°C/min, and then kept for 1 hour, and then continued to be heated to 2800°C at a rate of 5°C/min and kept for 30 minutes. Finally, after natural cooling to room temperature, the graphite film was obtained.

Regarding the naming of the samples: In this article, the PI film without the addition of catalyst is named PI; the PI film

with the addition of isoquinoline is named Y-x% (x is the addition amount of isoquinoline); the carbon film of pure PI is named C-PI; the PI-based carbon film with the addition of isoquinoline is named C-Yx% (x is the addition amount of isoquinoline); the PI-based graphite film is named G-Yx% (x is the addition amount of isoquinoline).

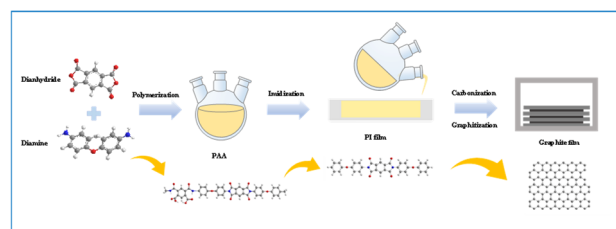


Figure 2. The preparation process of graphite film

### 2.3. Material characterization

The chemical structure, crystallinity, stress-strain behavior, thermal properties and glass transition temperature ( $T_g$ ) of the films were analyzed by Fourier transform infrared spectroscopy (FTIR, Perkin Elmer, Waltham, MA, USA), X-ray diffraction (XRD, Bruker, Bremen, Germany), material testing machine (ZwickRoell, Ulm, Germany), thermogravimetric analysis ( $T_g$ , Perkin Elmer) and differential scanning calorimetry (DSC, Netzsch, Hanau, Germany), respectively. The structures of carbonized and graphitized films were characterized by Raman spectroscopy (Horiba, Lille, France). The surface and cross-sectional morphologies of the films were observed by scanning electron microscopy (SEM, FEI Quanta FEG, FEI, Hillsboro, OR, USA) at an acceleration voltage of 20 kV.

### 2.4. Thermal conductivity test

The graphitized PI films were pressed into sheets by a tablet press, and the thermal diffusivity ( $\alpha$ ,  $\text{mm}^2\cdot\text{s}^{-1}$ ) was measured by a laser flash analyzer (LFA467 Nanoflash, Netzsch). During the measurement, each graphite film was automatically measured three times and the average value was taken. The error of  $\alpha$  was less than  $\pm 15 \text{ mm}^2\cdot\text{s}^{-1}$ . The thermal conductivity ( $\lambda$ ,  $\text{W}\cdot\text{m}^{-1}\cdot\text{K}^{-1}$ ) was calculated according to the literature by Equation (1).

$$\lambda = \rho \cdot C_p \cdot \alpha \quad (1)$$

Where  $\rho$  represents the density ( $\text{g}\cdot\text{cm}^{-3}$ , obtained by  $\rho = \text{m}\cdot\text{V}^{-1}$ , where  $\text{m}$  and  $\text{V}$  are the mass and volume of the sample respectively), and  $C_p$  represents the specific heat capacity ( $\text{J}\cdot\text{g}^{-1}\cdot\text{K}^{-1}$ ).

## 3. Results and Discussion

### 3.1. The structure and properties of PI films

Figure 3 shows the infrared spectra of the PI films prepared by adding isoquinoline. It can be seen from the infrared spectra that the PI films with the addition of chemical imidization reagents all have the characteristic absorption peaks of polyimide, including the asymmetric stretching vibration and symmetric stretching vibration of the carbonyl group in the imide ring observed at  $1780 \text{ cm}^{-1}$  and  $1720 \text{ cm}^{-1}$  respectively, the characteristic absorption peak of the benzene ring at  $1500 \text{ cm}^{-1}$ , the peak at  $1360 \text{ cm}^{-1}$  is the stretching vibration of the C-N bond, and the deformation vibration peak

of the imide ring at  $725\text{ cm}^{-1}$ . In addition, there are no absorption peaks of carboxyl and amide bonds at  $1550\text{ cm}^{-1}$  and  $1660\text{ cm}^{-1}$  for the PI films, indicating that the imidization degree of the PI films prepared under different ratios is relatively complete.

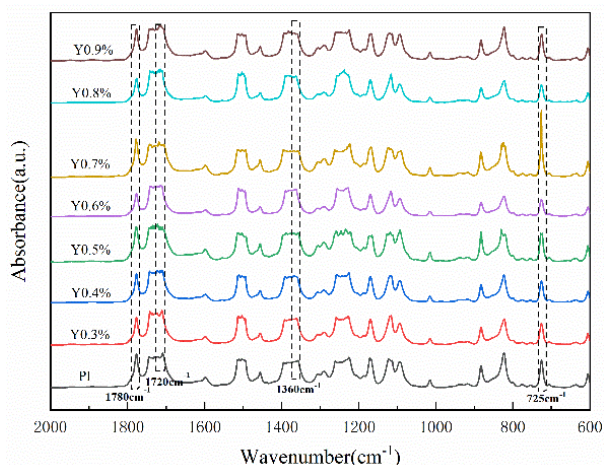


**Figure 3.** The Fourier transform infrared spectrum of PI films

**Figure 4** shows the stress-strain curves of PI films with different isoquinoline additions. With the addition of isoquinoline, the tensile strength of each PI film shows a trend of first increasing and then decreasing. According to the FTIR analysis, after the imidization reaction, the internal molecular structures of PI films with different additions are almost the same, and the difference in the tensile strength of each PI film may be caused by the difference in the aggregated structure of the films. When the addition amount of isoquinoline is 0.6%, the tensile strength of the PI film is 112 MPa, which is higher than that of pure PI (96 MPa). This indicates that the addition of an appropriate amount of isoquinoline promotes the imidization transformation of the PAA solution during the imidization process, reduces the molecular chain mobility,

makes the internal molecular chains of the prepared PI film arranged more regularly and neatly, and has a high in-plane orientation degree. Therefore, the mechanical properties of the corresponding PI film are more excellent. Excessive isoquinoline will affect the bonding force between PI molecular chains, resulting in a decrease in the mechanical properties of the film.

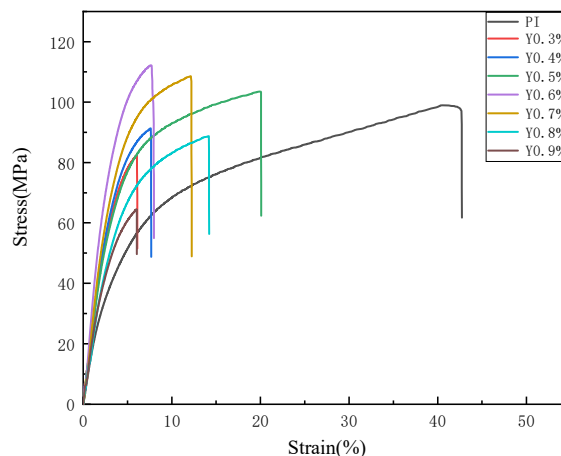


**Figure 4.** The stress-strain curves of PI films

**Figure 5** shows the TG and DTG curves of the PI film with an isoquinoline addition of 0.6% and the pure PI film. It can be seen from the figure that a slight weight loss occurs when the temperature is lower than  $300^\circ\text{C}$  in the early stage, and after  $500^\circ\text{C}$ , the PI film begins to undergo pyrolysis. **Figure 5(a)** is the curve of the pure PI film, and its fastest decomposition temperature is  $600^\circ\text{C}$ ; **Figure 5(b)** is the curve of the PI film with an isoquinoline addition of 0.6%, and its fastest decomposition temperature is  $609^\circ\text{C}$ . Thus, it can be seen that the addition of isoquinoline can effectively improve the thermal stability of the PI film.

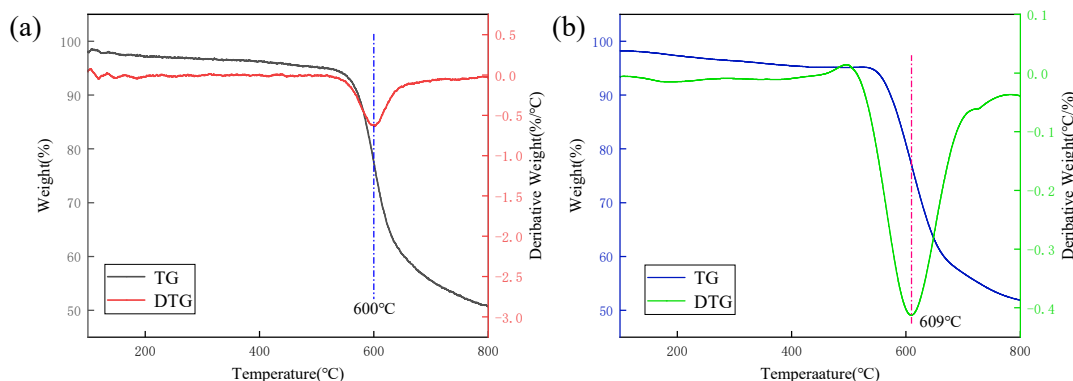


**Figure 5.** TG and DTG curves of PI films: (a) Pure PI film; (b) PI film with 0.6% isoquinoline added

### 3.2. The morphology and structure of PI-based carbon films and PI-based graphite films

**Figure 6** shows the structural test curves of PI-based carbon films prepared under different isoquinoline additions. It can be seen from the figure that each PI-based carbon film has a wide peak "mantou peak" near  $24.5^\circ$ , and the

crystallinity of the carbon film is low at this time. With the increase of the amount of isoquinoline added, the interplanar spacing of the PI-based carbon films first decreases and then increases. When the addition amount of isoquinoline is 0.6%, the interplanar spacing of the carbon film is the smallest, which is  $0.3599\text{ nm}$ . It indicates that when the addition amount of isoquinoline is 0.6%, the molecular weight of the

prepared polyamic acid increases significantly, and the order degree is significantly improved, which will effectively promote the growth of the highly oriented and dense graphite structure in the graphitization process.

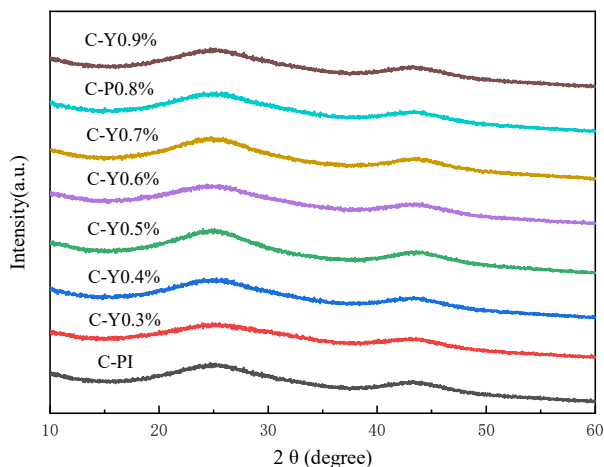


**Figure 6.** The structural test curves of PI-based carbon films prepared with different isoquinoline additions

**Figure 7** shows the Raman spectra of PI-based carbon films prepared with different isoquinoline additions. It can be seen from the figure that the D peak ( $1340 \sim 1360 \text{ cm}^{-1}$ ) and the G peak ( $1580 \sim 1590 \text{ cm}^{-1}$ ) appear in the Raman spectra. The films after carbonization treatment show "mantou peaks" at the D peak and the G peak, and the coincidence degree of the D peak and the G peak is high, indicating the formation of amorphous carbon. With the increase of the amount of isoquinoline added, the value of  $I_D/I_G$  shows a trend of first decreasing and then increasing, indicating that when the amount of isoquinoline is 0.6%, it is more conducive to the graphitization of the carbon film.

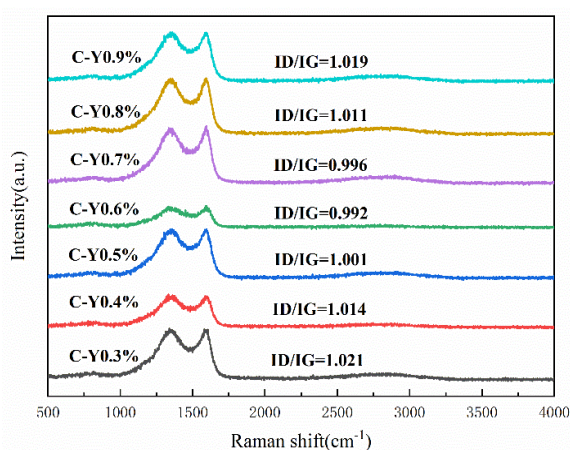


**Figure 7.** The Raman spectra of PI-based carbon films prepared with different isoquinoline additions

**Figure 8** shows the Raman spectra of graphite films prepared with different isoquinoline additions. After graphitization treatment, the decrease in the intensity of the D peak is the elimination of defects and the repair of the  $sp^2$  lattice structure. It indicates the high in-plane orientation of the graphite film and few defects. The  $I_D/I_G$  values of graphite films prepared with different additions indicate that during the graphitization process, the  $sp^3$  hybridization transforms into the  $sp^2$  hybridization structure, and the crystallinity increases.

It shows that the addition of isoquinoline accelerates the change of the molecular structure from  $sp^3$  hybridization to  $sp^2$  hybridization, reduces edge defects, and is conducive to the formation of an in-plane interlayer structure. When the addition amount is 0.6%, the  $I_D/I_G$  value of the graphite film is the smallest, which is 0.073, indicating that the addition of an appropriate amount of isoquinoline has a positive effect on the repair of the structural defects of the graphite film. In addition, the  $I_D/I_G$  ratio characterizes the degree of graphitization; the smaller the ratio, the higher the degree of graphitization. Since the D peak is almost non-existent in the Raman spectrum, the ratio is close to 0, indicating that the film after graphitization treatment has a high degree of graphitization.

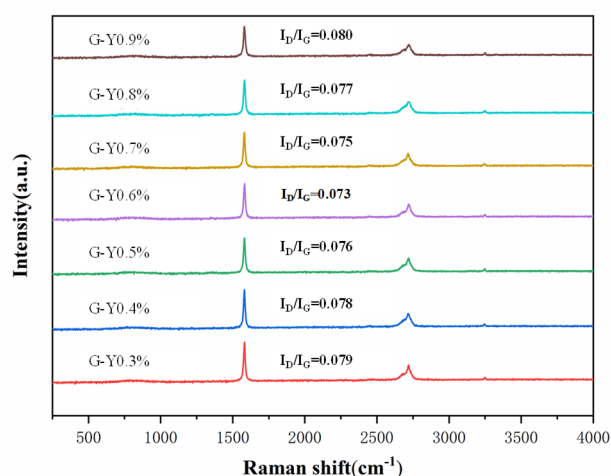


**Figure 8.** The Raman spectra of graphite films prepared with different isoquinoline additions

**Figure 9** shows the structural test curves of PI-based graphite films prepared with different isoquinoline additions. After graphitization, graphite diffraction peaks appeared in all XRD patterns of the films. The XRD diffraction peak at around  $26.5$  degrees corresponds to the (002) crystal plane in the graphite structure, and the small XRD diffraction peak at around  $54.6$  degrees corresponds to the (004) crystal plane. It indicates that with the progress of the graphitization reaction, the carbon layer structure of the film has been rearranged, and the crystallinity has increased. After the carbonization and graphitization treatment of the PI film, it has completely transformed into a graphite structure. With the addition of isoquinoline, the  $2\theta$  diffraction angle of the (002) crystal plane of the graphite film decreases, and its (002) peak becomes very sharp, indicating that during the transformation process from the carbon film to the graphite film, the grains gradually grow, and the film forms an ordered graphite structure. It indicates that the addition of isoquinoline is beneficial to improving the crystallinity and distribution orientation of the PI graphite film. In addition, among the films prepared with different additions, the interlayer spacing  $d_{002}$  of the G-Y0.6% sample is the smallest, which is  $0.3387 \text{ nm}$ . It indicates that a small amount of isoquinoline is beneficial to increasing the orderliness of the aggregated structure of the film and is closer to the theoretical single crystal.

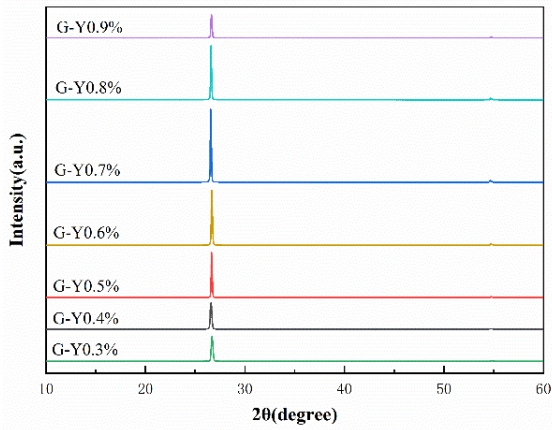


**Figure 9.** The structural test curves of PI-based graphite films prepared with different isoquinoline addition

**Figure 10** shows the SEM images of the cross-section of PI-based graphite films graphitized at 2800 °C. Judging from the cross-sectional morphology images of each PI-based graphite film shown in **Figure 10 (a-f)**, it can be observed that each cross-section has a layered structure characteristic and is neatly arranged. This layered structure has a strong orientation in the planar direction. This means that during the graphitization process of the carbon film, the molecular chains are rearranged and gradually form a graphite layer structure with regular arrangement, laying a good foundation for in-plane heat transfer. When the addition amount of isoquinoline is 0.6%, the cross-sectional layered structure is the densest and most ordered, which will reduce phonon scattering and improve thermal conductivity. This indicates that adding an appropriate content of isoquinoline is helpful to prepare high thermal conductivity graphite films with higher orientation, denseness and fewer defects.

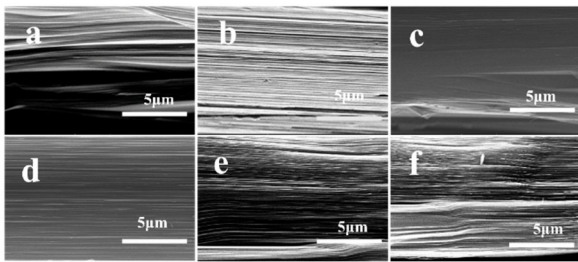


**Figure 10.** The SEM images of the cross-section of PI-based graphite films: (a) Pure PI-based graphite film; (b)G-Y0.4%; (c)G-Y0.5%;(d)G-Y0.6%; (e)G-Y0.7%;(f)G-Y0.8%

### 3.3. The thermal conductivity of PI-based graphite films

**Figure 11** shows the thermal conductivity analysis diagram of PI-based graphite films prepared with different isoquinoline additions. It can be seen from the figure that with the increase of the amount of isoquinoline added, the thermal conductivity of the graphite film first increases and then decreases, reaching the maximum value ( $1597 \text{ W}\cdot\text{m}^{-1}\cdot\text{K}^{-1}$ ) at 0.6%, which is higher than that of the pure PI-based graphite film ( $1331 \text{ W}\cdot\text{m}^{-1}\cdot\text{K}^{-1}$ ). These indicate that the addition of isoquinoline makes the layered structure of graphite more uniform and dense, reduces the defect concentration inside graphite, and is conducive to improving the thermal conductivity of graphite.

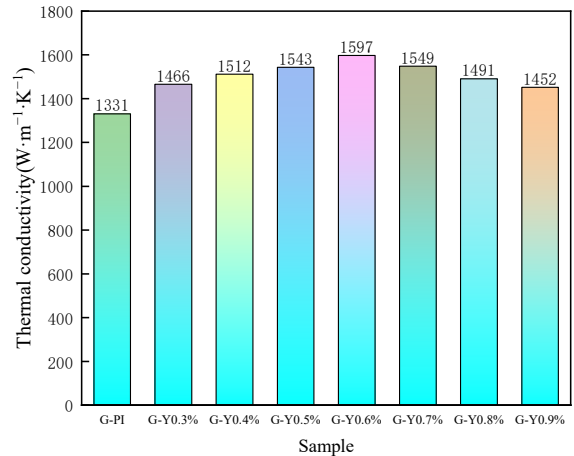


**Figure 11.** The thermal conductivity of graphite films

## 4. Conclusions

By adding catalytic imidization reagents during the polymerization process, PI films containing one or two catalytic imidization reagents were prepared, and their thermal properties, mechanical properties and aggregated structure were characterized and tested. In addition, PI-based graphite films were prepared by further carbonization and graphitization of PI films, and the influence of the addition amount and addition ratio of catalytic imidization reagents on their structure and properties was studied and analyzed. The basic conclusions are as follows:

(1) The preparation of PI films by the chemical imidization method can effectively improve the degree of imidization and the orderly arrangement of molecular chains inside the films. On the one hand, it is beneficial to the improvement of the mechanical properties of PI films. On the other hand, it is beneficial to the generation of regular and orderly crystalline graphite structures in the graphitization process.

(2) The addition amount of the catalytic imidization reagent isoquinoline was regulated to prepare seven kinds of PI films, and then high-temperature carbonization-graphitization treatment was carried out to obtain PI-based graphite films. When the addition amount of isoquinoline was 0.6%, the PI film had good thermal stability, and the thermal conductivity of the graphite film reached the maximum value of  $1597 \text{ W}\cdot\text{m}^{-1}\cdot\text{K}^{-1}$ , corresponding to a smaller interplanar spacing and a larger grain size, as well as a dense and orderly graphite stacking structure.

## References

- [1] Wang C X, Hua L J, Yan H Z, et al. A Thermal Management Strategy for Electronic Devices Based on Moisture Sorption-Desorption Processes [J]. *Joule*, 2020, 4(2): 435-447
- [2] Zhang B, Wang L W, Zhang C, et al. High-performance cellulose nanofiber-derived composite films for efficient thermal management of flexible electronic devices [J]. *Chemical Engineering Journal*, 2022, 439(1-9).
- [3] Bahru R, Hamzah A A, Mohamed M A. Thermal management of wearable and implantable electronic healthcare devices: Perspective and measurement approach [J]. *Int J Energy Res*, 2021, 45(2): 1517-1534.
- [4] He Z Q, Yan Y F, Zhang Z E. Thermal management and temperature uniformity enhancement of electronic devices by micro heat sinks: A review [J]. *Energy*, 2021, 216(1-38).

- [5] Alshaer W G, Nada S A, Rady M A, et al. Thermal management of electronic devices using carbon foam and PCM/nano-composite [J]. *Int J Therm Sci*, 2015, 89(79-86).
- [6] Li S Z, Zheng Z B, Liu S W, et al. Ultrahigh thermal and electric conductive graphite films prepared by g-C<sub>3</sub>N<sub>4</sub> catalyzed graphitization of polyimide films [J]. *Chemical Engineering Journal*, 2022, 430(1-11).
- [7] Chen J, Yao B W, Li C, et al. An improved Hummers method for eco-friendly synthesis of graphene oxide [J]. *Carbon*, 2013, 64(225-229).
- [8] Pei S, Cheng H. The reduction of graphene oxide [J]. *Carbon*, 2012, 50(9): 3210-3228.
- [9] Huang H G, Ming X, Wang Y Z, et al. Polyacrylonitrile-derived thermally conductive graphite film via graphene template effect [J]. *Carbon*, 2021, 180(197-203).
- [10] De Silva K K H, Huang H H, Joshi R, et al. Restoration of the graphitic structure by defect repair during the thermal reduction of graphene oxide [J]. *Carbon*, 2020, 166(74-90).
- [11] Liu Y H, Qu B X, Wu X E, et al. Utilizing ammonium persulfate assisted expansion to fabricate flexible expanded graphite films with excellent thermal conductivity by introducing wrinkles [J]. *Carbon*, 2019, 153(565-574).
- [12] Liu Y, Zeng J, Han D, et al. Graphene enhanced flexible expanded graphite film with high electric, thermal conductivities and EMI shielding at low content [J]. *Carbon*, 2018, 133(435-445).
- [13] Park H J, Meyer J, Roth S, et al. Growth and properties of few-layer graphene prepared by chemical vapor deposition [J]. *Carbon*, 2010, 48(4): 1088-1094.
- [14] Obratsov A N, Obratsova E A, Tyurnina A V, et al. Chemical vapor deposition of thin graphite films of nanometer thickness [J]. *Carbon*, 2007, 45(10): 2017-2021..
- [15] Kato T, Yamada Y, Nishikawa Y, et al. Carbonization mechanisms of polyimide: Methodology to analyze carbon materials with nitrogen, oxygen, pentagons, and heptagons [J]. *Carbon*, 2021, 178(58-80).
- [16] Suhng Y, Hashizume K, Kaneko T, et al. The study of the graphitization behavior for polyimide and polyamide films [J]. *Synthetic Metals*, 1995, 71(1): 1751-1752.
- [17] Bürger A, Fitzer E, Heym M, et al. Polyimides as precursors for artificial carbon [J]. *Carbon*, 1975, 13(3): 149-157.
- [18] Inagaki M, Ohta N, Hishiyama Y. Aromatic polyimides as carbon precursors [J]. *Carbon*, 2013, 61(1-21).
- [19] Inagaki M, Harada S, Sato T, et al. Carbonization of polyimide film “Kapton” [J]. *Carbon*, 1989, 27(2): 253-257.
- [20] Inagaki M, Meng L, Ibuki T, et al. Carbonization and graphitization of polyimide film “Novax” [J]. *Carbon*, 1991, 29(8): 1239-1243.
- [21] Inagaki M, Sakamoto K, Hishiyama Y. Carbonization and graphitization of polyimide Upilex [J]. *Journal of Materials Research*, 1991, 6(5): 1108-1113.
- [22] Inagaki M, Ibuki T, Takeichi T. Carbonization behavior of polyimide films with various chemical structures [J]. *Journal of Applied Polymer Science*, 1992, 44(3): 521-525.
- [23] Smirnova V E, Gofman I V, Maritcheva T A, et al. The effect of different orientations in rigid rod polyimide films on the graphitized products [J]. *Carbon*, 2007, 45(4): 839-846.
- [24] Zhong D H, Sano H, Kobayashi K, et al. A study of film thickness dependence of the graphitizability of PMDA-ODA polyimide-derived carbon film [J]. *Carbon*, 2000, 38(15): 2161-2165.
- [25] Inagaki M, Hishiyama Y, Kaburagi Y. Effect of heating rate during carbonization on graphitization of carbon films derived from aromatic polyimides [J]. *Carbon*, 1994, 32(4): 637-639.
- [26] Inagaki M, Sato M, Takeichi T, et al. Effect of constraint during imidization of polyamic acid films on graphitizability of resultant carbon films [J]. *Carbon*, 1992, 30(6): 903-905.
- [27] Nysten B, Issi J P, Shioyama H, et al. Effect of FeCl<sub>4</sub>-intercalation on the transport properties of a graphitized polyimide film [J]. *Journal of Materials Research*, 1993, 8(9): 2299-2304.
- [28] Konno H, Shiba K, Kaburagi Y, et al. Carbonization and graphitization of Kapton-type polyimide film having boron-bearing functional groups [J]. *Carbon*, 2001, 39(11): 1731-1740.